Low-latency RFI Nulling and Multi-user Scaling for 5G and Radio Astronomy Coexistence

Siddharth Dongre, Tiep M. Hoang, Hanif Rahbari, and Alireza Vahid
Rochester Institute of Technology, Rochester, NY
Email: {sd4767, tmheme, hanif.rahbari, alireza.vahid}@rit.edu

2025 IEEE 22nd Consumer Communications & Networking Conference (CCNC) | 979-8-3315-0805-0/25/$31.00 ©2025 IEEE | DOI: 10.1109/CCNC54725.2025.10976173

***Abstract*—5G network operators are constantly under pressure from regulatory agencies who restrict the deployment of base stations (gNBs) close to incumbent services, such as radio astronomy services (RAS), to avoid interfering with them. Recent works for coexistence with RAS employ limited channel modeling approaches and use explicit out-of-band communication between the gNB and RAS. However, the strict latency requirements of 5G make explicit communications less desirable due to their overheads. Deploying gNBs close to RAS is also not yet supported. In this paper, we propose a proactive open-loop beamforming and interference nullification technique in which a gNB nullifies its downlink signal at a nearby RAS telescope while beamforming to its users (UEs). We estimate the gNB-RAS channel using raytracing on open-source terrain maps. We formulate a problem that maximizes the minimum rate for UEs under the constraint of maximum allowable interference power at the RAS and show that its time complexity scales cubically with the number of gNB antennas. Hence, we propose a heuristic solution that achieves 4 orders better latency and 100 dBW lower interference power than the max-min rate solution with similar sum rate on users. Our proposed solution consistently achieves less than -310 dBW interference power, even when the gNB-RAS distance is less than 1 km, satisfying international regulations, and is robust against moving users that vary in location and elevation.**

***Index Terms*—5G, RAS, nullification, coexistence.**

I. Introduction

5G cellular operators are pushing for more efficient, smarter, and geographically widespread base stations (a.k.a. gNBs) to deliver ubiquitous, high-speed, and low-latency services [1], [2]. Although expanding network coverage is attractive for the operators, deployments in new geographic regions still have to abide by the radio frequency interference (RFI) regulations mandated by regulatory agencies, such as the Federal Communications Commission (FCC), and ensure that nearby incumbent systems, such as radio astronomy services (RAS), are unaffected. Extremely strict regulations which include interference limits of -220 dBW pose a challenge for network operators [3]. The proliferation of emerging coexistence protocols, such as 5G New Radio Unlicensed, has also led to a significant increase in RFI by gNBs now in the 5–7 GHz bands, which overlap with the 0–10 GHz bands used by RAS telescopes, causing substantial damage to astronomical observations [4]. If the RFI regulations are violated, sanctions can be placed on 5G operators by the FCC [5]. Hence, there is a need to develop a fair and compliant coexistence mechanism that allows 5G operators to coexist with RAS observatories.

National Radio Dynamic Zones (NRDZs) have been recently proposed to aid RAS-coexistence research efforts in the United States. These zones employ large-scale experimental testbeds to enable spectrum-sharing research and real-world validation of, among others, 5G and RAS coexistence schemes [6]. These NRDZs work well with RAS telescopes that operate at almost 100% duty cycles across a wide range of frequencies, including 0–10 GHz. However, they require 5G operators to remain within interference threshold boundaries, especially for gNBs located close to the edges of the zones which pose a big challenge [6]. Moreover, NRDZs do not yet cover observatories that only have access to small single-dish telescopes of less than 4 m diameter, such as the "KROC" telescope located in Ionia, NY, that is affected by gNBs within 10 km [7]. Due to such limitations, we argue that an alternative method where gNBs could proactively nullify their interference at the location of the RAS observatories using carefully designed precoding techniques would be more effective. In practice, however, implementing such nullification schemes is challenging since they need to (1) work with passive receivers that themselves do not provide any *explicit* feedback for channel state information (CSI) carrying information about, for example, terrain reflections, (2) limit the unintentional negative effects on their users (UEs), (3) satisfy strict latency requirements of 5G, and (4) support widespread deployment of gNBs in areas close to RAS.

A gNB may estimate the channel based on limited CSI feedback using techniques such as channel covariance models as features for deep learning frameworks [8] or using the angle of arrival and departure information for deriving CSI [9]. However, these techniques are insufficient for modeling channels that also involve terrain reflections, which may not be strong enough to severely impact UEs, but significantly contribute to interference on RAS telescopes. To limit the negative effects of nullification on UEs, interference broadcast channels have been proposed but with drawbacks. For example, techniques that determine CSI using Gaussian-like interference channel models cannot accurately implement terrain reflections [10]. Alternatively, explicit channel coordination schemes have also been proposed that do not require the exchange of CSI, such as those that send stochastic characteristics of the downlink signals via out-of-band links [4], [11], or use intelligent reflecting surfaces to mitigate RFI [12]. However, they may be

The work of A. Vahid was in part supported by NSF grants CNS-2343964 and AST-2348589. Any opinions, findings, and conclusions are the author(s)' and may not reflect the views of the NSF.

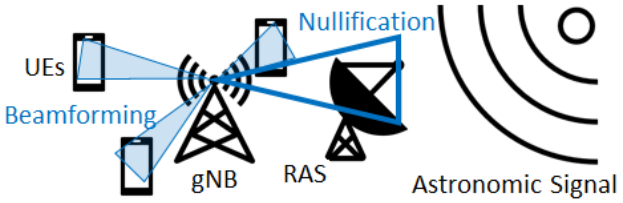

Fig. 1. 5G and RAS coexistence in a nutshell.

challenging to implement in 5G due to the latency overhead of using explicit communication links, which is undesirable for ultra-reliable and low-latency applications of 5G that require latency of less than 0.5 ms [13]. Besides the above limitations, none of the existing works have simultaneously addressed all the challenges mentioned above and they do not support a gNB placed close, within 1 km, of an RAS telescope which would help cellular network providers expand their coverage.

In this paper, we propose a coexistence mechanism that addresses all the above challenges and provides 5G network operators the means to satisfy RFI regulations and latency constraints of 5G even when deploying the gNB close to the RAS telescope or NRDZ. To the best of our knowledge, we are the first to propose an entirely proactive nullification scheme that does not require any explicit CSI exchange between the gNB and RAS (although it can support the addition of external sensors to help with CSI estimation).

To achieve our goal, we first formulate a problem to maximize the sum rate of the UEs of a given gNB, which we then simplify into a max-min fair rate problem, subject to the constraint of interference power at the RAS telescope being less than -220 dBW. Due to the high computational complexity of this problem, which scales cubically with the number of gNB antennas, we propose a novel heuristic solution that leverages the channel between the gNB and RAS telescope, determined through a coarse channel estimation technique. Our idea is to use raytracing methods, operating on open-source terrain data obtained from OpenStreetMap [14], as a tool to determine information on rays of propagation paths of the gNB's signals between the gNB and RAS telescope locations. These rays contain the angle of arrival and departure, path delays, and path gain information used to define the CSI between the gNB and RAS telescope. As shown in Fig. 1, we use this channel information to derive a carefully chosen heuristic to beamform the gNB downlink signal on UEs, achieving a sum rate that is comparable to the max-min fair solution while satisfying the interference power constraint. Our proposed solution consistently reduces the interference power at the RAS to less than -310 dBW under most common gNB operating parameters, even when the gNB is within 1 km of the RAS telescope, with a similar sum rate of UEs while being 4 orders of magnitude faster in latency compared to the max-min fair solution. We show that our scheme is also robust against moving UEs that vary their location and elevation.

The rest of the paper is organized as follows. In Section II we provide a primer on RAS and raytracing for channel modeling. We then describe our open-loop beamforming and interference nullification technique in detail in Section III. The performance evaluation of our proposed technique is provided in Section IV before concluding the paper in Section V.

II. Background and System Model

We first provide an overview of RAS systems, followed by raytracing methods and a description of the 5G and RAS coexistence system model used in our paper.

A. Radio Astronomy Services

Ground-based RAS stations observe deep space objects using low-frequency radio waves ranging from 0–10 GHz [15]. At these frequencies, RAS telescopes are looking for electron transitions in hydrogen atoms that can help locate distant celestial objects. These low-frequency radio waves, with wavelengths spanning from a few meters to several kilometers, can penetrate through dense clouds of gas and dust that obstruct visible light, enabling ground telescopes to observe celestial objects and phenomena that would otherwise remain concealed. Radio telescopes, designed to detect these radio waves, are typically situated in remote locations to minimize RFI from external sources, such as gNBs, and keep the interference power of RFI sources below -220 dBW at the RAS telescope.

B. Raytracing Methods

The shooting-and-bouncing rays (SBR) method of raytracing is used to determine the propagation paths of the downlink signal between the gNB and the RAS telescope. This method involves backtracking by generating rays from the intended receiver, *i.e.*, the RAS telescope, and tracing the rays as they reflect off of objects and terrain in the environment. After backtracking, the rays that reach the gNB are the propagation paths of the downlink signal. The total number of possible propagation paths is controlled by assigning a maximum number of ray reflections, R, which limits the number of reflections a ray will make before it reaches the gNB. A ray that has undergone signal attenuation of greater than -130 dB before it reaches the receiver is considered to be terminated.

C. System Model

In our 5G and RAS coexistence system, we assume the gNB has M omnidirectional dipole antennas serving K UEs. All UEs are less than 100 m away from the gNB. The gNB transmits on carrier frequency f_c within the FR1 frequency bands of up to 7.125 GHz. We consider a single-dish telescope that is 2 m high and between 100 m and 12 km away from the gNB with one parabolic antenna operating in the $0-10$ GHz range. The CSI between the gNB and the kth UE is denoted by $\mathbf{h}_k$ and that between the gNB and RAS is denoted by $\mathbf{h}_{gR}$. Note that $\mathbf{h}_k$ and $\mathbf{h}_{gR}$ are time-variant, but we omit the dependency on time since the channels are updated after each 1 ms 5G subframe when the gNB executes channel estimation.

III. Open-loop Beamforming and Interference Nullification

In this section, we first formulate our problem to optimize the rate for UEs under an interference power constraint at the RAS. We then describe our raytracing approach to estimate the gNB-RAS channel, followed by our highly efficient heuristic solution to achieve our objective.

A. Problem Formulation

In this paper, we primarily consider RFI from the downlink signal of one gNB. We first consider the optimization problem (P1) to find the precoder $\mathbf{w}$ that maximizes the sum rate for K UEs while under a maximum allowable interference power constraint at the RAS telescope, as shown below:

$$\max_{\mathbf{w}\in\mathbb{C}^{1\times M}} \sum_{k=1}^{K} \log_2\left(1+\frac{|\mathbf{h}_k\mathbf{w}^{\mathbf{H}}|^2}{\sigma_k^2}\right) \tag{P1}$$

$$\text{s.t. } |\mathbf{h}_{gR}\mathbf{w}^{\mathbf{H}}|^2 \le \epsilon,\ \epsilon>0 \tag{1}$$

$$0<\|\mathbf{w}\|^2\le\rho_b \tag{2}$$

where ρ_b is the beamforming power budget at the gNB, σ_k^2 is the noise power at the kth UE, and ϵ is the maximum allowable interference power at the RAS telescope.

The objective function in (P1) is non-convex. To simplify it, we assume the noise power σ_k^2 of each of the K UEs remains constant and convert the sum of logarithm terms into a logarithm of the product of $|\mathbf{h}_k\mathbf{w}^{\mathbf{H}}|^2$ terms, followed by removing the $\log_2()$ function entirely since the $|\mathbf{h}_k\mathbf{w}^{\mathbf{H}}|^2$ terms are monotonically increasing. Hence, we get the equivalent sum rate maximization problem as shown below:

$$\max_{\mathbf{w}\in\mathbb{C}^{1\times M}} \prod_{k=1}^{K} |\mathbf{h}_k\mathbf{w}^{\mathbf{H}}|^2 \tag{P2}$$

$$\text{s.t. } |\mathbf{h}_{gR}\mathbf{w}^{\mathbf{H}}|^2 \le \epsilon,\ \epsilon>0 \tag{3}$$

$$0<\|\mathbf{w}\|^2\le\rho_b. \tag{4}$$

The problem in (P2) is NP-hard since it requires simultaneously maximizing each quadratic term in the product [16]. We argue that a suboptimal solution to (P2) can be obtained by solving an alternate problem where we maximize the minimum of $|\mathbf{h}_k\mathbf{w}^{\mathbf{H}}|^2$ across all K users, as shown below:

$$\max_{\mathbf{w}\in\mathbb{C}^{1\times M}} \min_{k\in\{1,\dots,K\}} |\mathbf{h}_k\mathbf{w}^{\mathbf{H}}|^2 \tag{P3}$$

$$\text{s.t. } |\mathbf{h}_{gR}\mathbf{w}^{\mathbf{H}}|^2 \le \epsilon,\ \epsilon>0 \tag{5}$$

$$0<\|\mathbf{w}\|^2\le\rho_b. \tag{6}$$

The problem in (P3) is similar to a Max-Min fair beamforming problem, such as the one in [17], with the added maximum allowable interference constraint. Although the solution to (P3) is suboptimal to (P2), (P3) is solvable in polynomial time. For this, we use the Semidefinite Relaxation method as follows:

$$\max_{\mathbf{W}\in\mathbb{C}^{M\times M}} \min_{k\in\{1,\dots,K\}} \mathbf{Tr}(\mathbf{H}_k\mathbf{W}) \tag{P4}$$

$$\text{s.t. } \mathbf{Tr}(\mathbf{H}_{gR}\mathbf{W}) \le \epsilon,\ \epsilon>0 \tag{7}$$

$$0<\mathbf{Tr}(\mathbf{W})\le\rho_b, \mathbf{W}\succeq 0 \tag{8}$$

where $\mathbf{W}=\mathbf{w}^{\mathbf{H}}\mathbf{w}, \mathbf{H}_k=\mathbf{h}_k{}^{\mathbf{H}}\mathbf{h}_k, \mathbf{H}_{gR}=\mathbf{h}_{gR}{}^{\mathbf{H}}\mathbf{h}_{gR}$. Note that we have dropped the $\mathrm{rank}(\mathbf{W})=1$ constraint to relax (P4) into a semidefinite program and $\mathbf{W}\succeq 0$ denotes that the matrix $\mathbf{W}$ is positive semidefinite. We can further introduce an auxiliary variable τ and remove the minimization problem in (P4) while also converting the outer maximization problem into a minimization one as shown below:

$$\min_{\mathbf{W}\in\mathbb{C}^{M\times M},\tau\in\mathbb{R}} -\tau \tag{P5}$$

$$\text{s.t. } \mathbf{Tr}(\mathbf{H}_k\mathbf{W})\ge\tau,\quad \forall k\in\{1,\dots,K\} \tag{9}$$

$$\mathbf{Tr}(\mathbf{H}_{gR}\mathbf{W})\le\epsilon,\quad \epsilon>0 \tag{10}$$

$$0<\mathbf{Tr}(\mathbf{W})\le\rho_b,\quad \mathbf{W}\succeq 0 \tag{11}$$

The problem in (P5) is solvable because it involves minimizing a convex objective function with convex constraints. Due to the impracticality of deriving a closed-form solution to (P5), we use analytical solvers such as CVX, a package for specifying and solving convex optimization problems [18], [19]. However, the worst-case time complexity of (P5) is $\mathcal{O}(KM^3)$, which is still significant for when $M\approx K$. Hence, in the following sections, we develop a heuristic solution with a lower computational complexity and nullification at the RAS telescope, and a comparable sum rate for the UEs, while addressing challenges such as estimating the $\mathbf{h}_{gR}$ channel without explicit channel feedback.

B. Coarse Estimation of $\mathbf{h}_{gR}$

To estimate $\mathbf{h}_{gR}\in\mathbb{C}^{1\times M}$, we need the path delays, the path gains, and the angles of arrival and departure (azimuth and zenith directions) for all the signal propagation paths originating at the M antennas of the gNB and terminating at the RAS telescope's receiver. The SBR method (see Section II-B) is used to populate these parameters for each signal path from each of the M antennas. For this, only the geographical locations of the gNB and RAS are needed, along with access to open-source terrain maps like OpenStreetMap. The locations of the gNB and RAS are initialized in the terrain maps and the terrain data is used to evaluate rays between the gNB and RAS, assuming R maximum number of ray reflections. These rays involve reflections from the ground and nearby buildings, if any. Once the rays have been evaluated, path parameters from these rays can be extracted using the `raytrace()` function of MATLAB's Communication Toolbox.

The extracted path parameters can then be used to create an NR Clustered Delay Line (CDL) channel delay profile which can then provide a coarse channel estimate for $\mathbf{h}_{gR}$, using the `nrcdlChannel()` channel object of MATLAB's 5G Toolbox based on 5G specifications [20]. Although this channel estimate is not dynamic, it provides a coarse estimate sufficient for nullifying the gNB downlink signal at the RAS. This is because the primary components (due to line-of-sight) of this course channel estimate dominate other components (for example, due to reflections) by at least one order of magnitude. A detailed analysis of the sensitivity of our scheme to channel estimation error is left for future work.

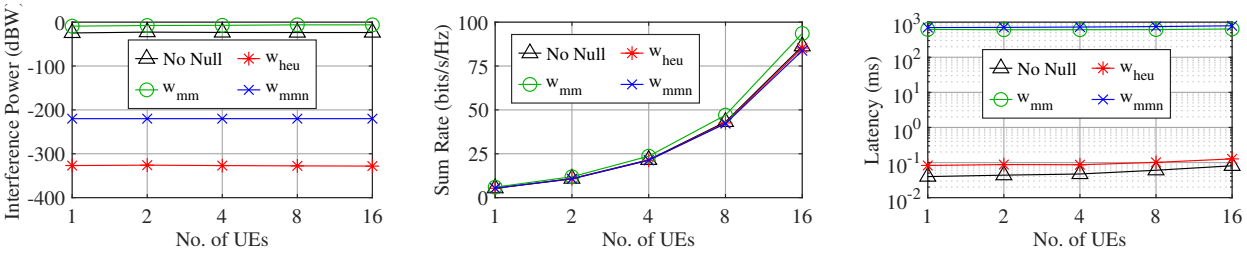

(a) Interference Power at RAS. (b) Sum rate over all UEs. (c) Latency of beamformer.

Fig. 2. Comparing the max-min rate solution $\mathbf{w}_{mmn}$ (w/ RAS null), $\mathbf{w}_{mm}$ (w/o RAS null), and our heuristic $\mathbf{w}_{heu}$ for K UEs.

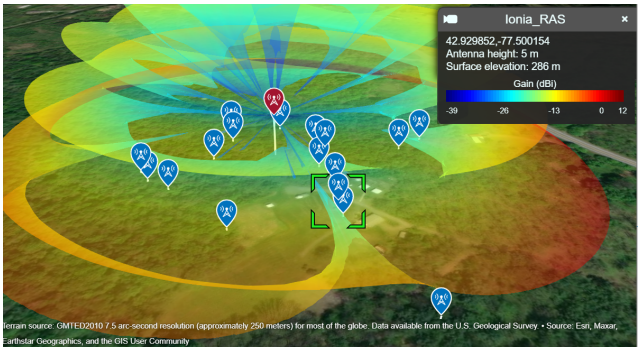

Fig. 3. Radiation pattern of the gNB when using our heuristic solution. The red pin indicates the location of the simulated gNB, the blue pin for the RAS telescope is highlighted in the center, and the remaining blue pins are the locations of simulated UEs.

C. Heuristic Solution to Nullify The gNB Signal at RAS

We assume the gNB uses linear precoding, such as the zero-forcing precoding technique to nullify the gNB interference at points of interest by projecting the downlink signal onto the null space of those points [13]. Similarly, we define the precoding scheme $\mathbf{w}_{null} \in \mathbb{C}^{1\times M}$, which only nullifies the gNB downlink signal at the RAS but does not simultaneously beamform on the UEs. Let $\mathbf{P}$ denote the orthonormal basis for the null space of the $\mathbf{h}_{gR}$ channel. Hence, $\mathbf{h}_{gR}\mathbf{P}\mathbf{P}^{\mathbf{H}} = \mathbf{0}$. When the precoding vector $\mathbf{w}_{null}$ is a member of the subspace $\mathbf{P}$ and is applied to the gNB downlink signal, it will ensure that the signal's null region overlaps with the location of the RAS telescope. Hence, we define $\mathbf{w}_{null}$ as,

$$\mathbf{w}_{null} = c\mathbf{v}_{gR}\mathbf{P}\mathbf{P}^{\mathbf{H}} \tag{12}$$

where $\mathbf{v}_{gR} \in \mathbb{C}^{1\times M}$ contains the singular vectors of the $\mathbf{h}_{gR}$ channel and c is any scalar. We can see that the constraint (5) is satisfied since $\mathbf{P}$ is in the null space of $\mathbf{h}_{gR}$ and $\mathbf{h}_{gR}\mathbf{w}_{null}^{\mathbf{H}} = \mathbf{h}_{gR}\mathbf{P}\mathbf{P}^{\mathbf{H}}\mathbf{v}_{gR}^{\mathbf{H}} = 0$. The precoding scheme $\mathbf{w}_{null}$ will perfectly nullify the gNB at the RAS, however, it may also harm some of the UEs by inadvertently nullifying UE locations. Hence, we slightly modify (12) as shown below,

$$\mathbf{w}_{heu} = c\mathbf{v}_{gU}\mathbf{P}\mathbf{P}^{\mathbf{H}} \tag{13}$$

where $\mathbf{v}_{gU} \in \mathbb{C}^{1\times M}$ contains the singular vectors of the channel matrix $\mathbf{H}_{gU} = [\mathbf{h}_1^{\mathbf{T}}; \mathbf{h}_2^{\mathbf{T}}; ...; \mathbf{h}_K^{\mathbf{T}}]$ containing the channel vectors to all the K UEs. The expression for $\mathbf{w}_{heu}$ in (13) satisfies the constraint in (5) since $\mathbf{h}_{gR}\mathbf{P}\mathbf{P}^{\mathbf{H}} = \mathbf{0}$, and hence is a valid solution for (P5). Although not an optimal solution, the worst-case time complexity of our proposed solution $\mathbf{w}_{heu}$ in (13) is $\mathcal{O}(M^2)$, which is better than that of (P5) by a factor of KM when using analytical solvers.

IV. Performance Evaluation

In this section, we compare our heuristic solution with the optimal one, then measure the change in gNB interference power at the RAS telescope, the change in SNR for a moving UE, and the latency of our beamforming algorithm.

1) Simulation Setup: We evaluate the performance of our beamforming algorithm by running simulations in MATLAB on an 8-core CPU with parallel processing capabilities. We implement the coarse channel estimation technique described in Section III-B. We assume $R = 1, 2, 3$ maximum number of ray reflections. To estimate the channels between the gNB and the K UEs, we implement CSI-RS and CSI Feedback messages sent by the gNB and UEs respectively. The gNB can have $M = \{4, 8, 16\}$ antennas transmitting at $f_c = \{0.7$ GHz, 1.8 GHz, 5.9 GHz$\}$ carrier frequencies, and supporting $K = \{1, 2, 4, 8, 16\}$ UEs. The distance between the gNB and the RAS telescope varies between 100 m and 12 km. We run $10,000$ unique iterations for each combination of gNB-RAS distance, M, f_c, K, and R for an extensive performance evaluation. Our simulations assume a real RAS observatory, "KROC" [7], located at the Max Farash Center for Observational Astronomy in Ionia, NY. We define this RAS telescope in all our MATLAB simulations, which remains constant, and randomize gNBs and UEs at simulated locations around it. In Fig. 3, we show the beam pattern of our proposed heuristic solution $\mathbf{w}_{heu}$ for one of the simulation runs, where the red pin indicates the location of the simulated gNB, less than 1 km from the RAS telescope (the highlighted pin), and the remaining blue pins are the locations of simulated UEs. We can see that our proposed solution $\mathbf{w}_{heu}$ nullifies at the location of the RAS telescope.

2) Heuristic vs. Max-Min Rate Solution: To prove the effectiveness of our proposed heuristic solution, we compare, (a) the beamformer used by gNBs in practice which does not nullify the RAS telescope by default, denoted by "No Null", (b) our proposed heuristic solution $\mathbf{w}_{heu}$, (c) the solution to problem (P5), denoted by $\mathbf{w}_{mmn}$, and (d) the solution to problem (P5) but without the RAS interference limit constraint in (10), denoted by $\mathbf{w}_{mm}$. We set $M = 16$, $f_c = 1.8$ GHz, $R = 3$ and $K = \{1, 2, 4, 8, 16\}$. In Fig. 2 (a), we can see

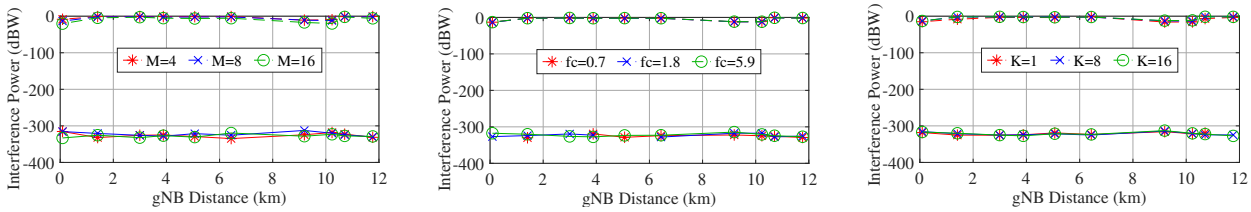

(a) $f_c = 5.9$ GHz, $R = 3$, $K = 16$. (b) $M = 16$, $R = 3$, $K = 16$. (c) $M = 16$, $f_c = 5.9$ GHz, $R = 3$.

Fig. 4. Interference power of the gNB at the RAS telescope with and without nullification, plotted in solid and dashed lines, respectively, while varying the gNB-RAS distance and the parameters M, f_c and K.

that the interference power achieved by $\mathbf{w}_{heu}$ is more than 100 dBW lower than $\mathbf{w}_{mmn}$. This is because $\mathbf{w}_{heu}$ is in the null space of $\mathbf{h}_{gR}$, bringing $|\mathbf{h}_{gR}\mathbf{w}^{\mathbf{H}}|^2$ very close to zero. Additionally, as seen in Fig. 2 (b), the sum rate for both $\mathbf{w}_{heu}$ and $\mathbf{w}_{mmn}$ is comparable to when there is no nullification being performed. This shows that both $\mathbf{w}_{heu}$ and $\mathbf{w}_{mmn}$ are acceptable solutions. Note that the sum rate when performing no nullification is indeed less than $\mathbf{w}_{mm}$, since in practice gNBs use a closed-form solution, based on singular value decomposition of the UE channels, instead of a slower, optimal one due to strict latency constraints [13]. In fact, as seen in Fig. 2 (c), the latency of $\mathbf{w}_{heu}$ is consistently less than 0.5 ms, while that of $\mathbf{w}_{mm}$ and $\mathbf{w}_{mmn}$ is more than 1000 ms, 4 orders of magnitude higher, which shows that our proposed solution $\mathbf{w}_{heu}$ is significantly faster. Considering these results, we argue that our proposed heuristic solution $\mathbf{w}_{heu}$ is more practical and effective than the max-min rate solution, and hence we use only $\mathbf{w}_{heu}$ to evaluate the following results.

3) Interference Power: In Fig. 4, we plot the interference power of the gNB at the RAS telescope versus increasing gNB-RAS distance and M to show their effect on the performance of our scheme. The dashed and solid lines denote default no nullification and heuristic solution, respectively. Our proposed solution incurs at most -300 dBW interference power at the RAS telescope for all gNB-RAS distances, while it varies between -350 – -310 dBW for varying M, f_c and K. In our set of simulations, with the gNB is less than 1 km away, the interference power was the highest at -312 dBW for $M = 8$ antennas, $f_c = 5.9$ GHz, $R = 3$ ray reflections and $K = 16$ UEs. This shows that our scheme meets the RAS interference constraint in (10) for most practical cases of gNB-RAS distance and M. Additionally, our nullification scheme performs well even in an edge case with $K = 8$ UEs surrounding the RAS telescope in a circle with 1 m radius, where the interference power is observed to be -333 dBW, with a total sum rate of 28 bits/s/Hz, compared to no nullification getting -37 dBW interference power and 36 bits/s/Hz sum rate.

4) Moving UEs: In Fig. 5, we plot the SNR at a moving UE to analyze the impact of changing the height and location of UEs on our scheme. We test three cases of moving UEs: (1) UE starts at the same latitude and longitude as the RAS telescope and moves vertically to heights $2, 4, 8, ..., 1024$ m, (2) UE starts at a random latitude and longitude that is within 100 m radius of the gNB and moves vertically similar to case 1, and (3) UE starts at a random location within 100 m of

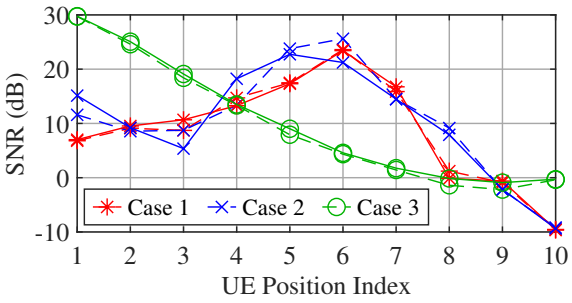

Fig. 5. SNR at a single moving UE that is varying its direction and elevation with and without nullification, plotted in solid and dashed lines, respectively, versus UE position index.

the gNB at 30 m height and moves northward (increasing latitude) at increments of 10 m. Case 1 analyzes how close a UE can get to the RAS telescope without adversely affecting our scheme, while cases 2 and 3 show that our scheme can support UEs moving in both vertical and horizontal directions, respectively. Solid lines represent nullification at RAS, while dashed is for a default beamformer. Firstly, the dashed and solid lines have similar results for all cases, showing that our proposed heuristic solution is robust against moving UEs. For case 1, we see that the moving UE still has about 9 dB SNR even within 1 m of the RAS telescope, as per position index 2 (the height of the telescope is 5 m), showing that our scheme works fairly well even when UEs are close to the RAS telescope. Note the SNR decreases as the UE moves from position index 1 to 3 since it is moving closer to the RAS, then the SNR starts increasing again from index 4 onwards as it starts moving away. We see a similar trend for case 2, with an SNR difference of 0–10 dB between cases 1 and 2, showing that the starting position of the moving UE does not significantly impact the change in its SNR as the UE increases its height. Also, for case 3, the UE moving northward has similar SNR with and without using the precoding scheme from our proposed solution. Note that the decrease in SNR for increasing UE index, in all cases, is due to the increase in distance between the gNB and the UE.

5) Latency: To show that our proposed scheme satisfies the latency requirements of 5G, in Fig. 6, we plot the latency of our proposed beamforming and interference nullification algorithm, where we observe that the latency is within 0.5 ms for all the gNB operating parameters that we tested. Latency is measured by observing the current system time before and

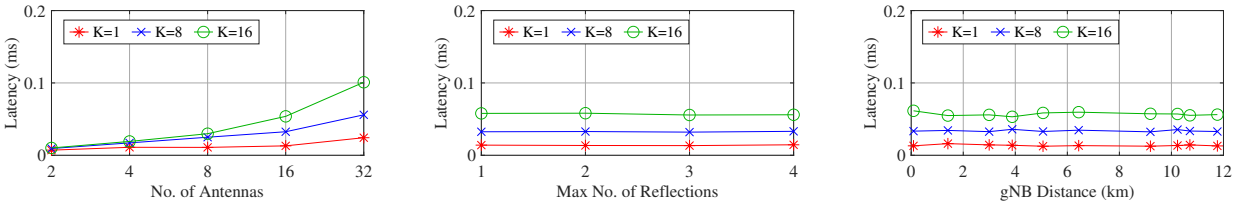

(a) Dist.= 1 km, $f_c = 5.9$ GHz, $R = 3$. (b) Dist.= 1 km, $M = 16$, $f_c = 7$ GHz. (c) $M = 16$, $f_c = 2.4$ GHz, $R = 3$.

Fig. 6. Latency of our scheme while varying the parameters M, R, K, and the gNB-RAS distance.

after executing the equation (13). In Fig. 6 (a), we observe that the latency of our proposed scheme increases with M and K for constant gNB-RAS distance of 1 km, $f_c = 5.9$ GHz, and $R = 3$, since M and K are the dimensions of the channel matrix $\mathbf{H}_{gU}$ directly controlling the computational complexity of our algorithm. In Fig. 6 (b), we observe that the latency is unaffected by the maximum number of ray reflections, R, for constant gNB-RAS distance of 1 km, $M = 16$ and $f_c = 7$ GHz. This is because the ray tracing algorithm used to determine a coarse estimate of the gNB-RAS channel, $\mathbf{h}_{gR}$, needs to be run only once. Once the gNB has the $\mathbf{h}_{gR}$ channel, it can use the same channel object for all subsequent precoder computations, unless there are significant changes in the terrain and environment between the gNB and RAS. Hence, it does not affect the latency of our scheme. Finally, in Fig. 6 (c), we see that the latency of our proposed scheme is mostly unaffected when increasing the gNB-RAS distance for constant $M = 16$, $f_c = 2.4$ GHz, and $R = 3$.

V. Conclusion and Future Work

In this paper, we have developed a proactive and open-loop beamforming and interference nullification scheme to facilitate 5G and RAS coexistence. We have formulated a problem to maximize the minimum rate for UEs under an interference power constraint of -220 dBW at the RAS telescope. We then propose a highly efficient heuristic solution, based on singular vector decomposition, whose time complexity is better than the max-min rate evaluation by a factor of KM. We have also shown that our proposed solution has a similar sum rate for UEs when compared to the max-min solution while achieving more than 100 dBW lower interference power at the RAS and a latency that is 4 orders of magnitude faster. Through extensive simulations, we have shown that our proposed solution consistently achieves less than -310 dBW interference power at the RAS, even when the gNB is less than 1 km from the RAS telescope, and is robust against moving UEs that vary their location and elevation. For future work, we plan to experimentally evaluate our scheme and improve our heuristic solution to nullify the entire surface of the RAS telescope antenna and improve the robustness of our technique against errors in channel estimation using open-source terrain data.

References

[1] D. Qiu, M. Lavergne, A. Samba, H. Afifi, and Y. Gourhant, "Machine learning for estimating the impact of adding new mobile network cells," in *IEEE Global Commun. Conf.*, Dec. 2023, pp. 6109–6114.

[2] M. Filo, C. H. Foh, S. Vahid, and R. Tafazolli, "Performance analysis of ultra-dense networks with regularly deployed base stations," *IEEE Trans. Wireless Commun.*, vol. 19, no. 5, pp. 3530–3545, May 2020.

[3] International Telecommunications Union Radiocommunication Sector (ITU-R). (2003) Recommendation ITU-R RA.769. [Online]. Available: https://tinyurl.com/3kdjuxe5

[4] S. Chakraborty, G. Hellbourg, M. Careem, D. Saha, and A. Dutta, "Collaboration with cellular networks for RFI cancellation at radio telescope," *IEEE Trans. on Cogn. Commun. Netw.*, vol. 9, no. 3, pp. 765–778, Jun. 2023.

[5] FCC Enforcement Bureau. (2020) Enforcement overview. [Online]. Available: https://tinyurl.com/mux57ppz

[6] M. Zheleva, C. R. Anderson, M. Aksoy, J. T. Johnson, H. Affinnih, and C. G. DePree, "Radio dynamic zones: Motivations, challenges, and opportunities to catalyze spectrum coexistence," *IEEE Commun. Mag.*, vol. 61, no. 6, pp. 156–162, Jun. 2023.

[7] M. Pepe. (2020) ART - autonomous radio telescope - ASRAS. [Online]. Available: https://tinyurl.com/yarn7a47

[8] A. M. Elbir, "A deep learning framework for hybrid beamforming without instantaneous CSI feedback," *IEEE Trans. Veh. Technol.*, vol. 69, no. 10, pp. 11 743–11 755, Oct. 2020.

[9] P. N. Alevizos, X. Fu, N. D. Sidiropoulos, Y. Yang, and A. Bletsas, "Limited feedback channel estimation in massive MIMO with non-uniform directional dictionaries," *IEEE Trans. Signal Process.*, vol. 66, no. 19, pp. 5127–5141, Oct. 2018.

[10] M. Zohdy, A. Tajer, and S. Shamai, "Distributed interference management: A broadcast approach," *IEEE Trans. Commun.*, vol. 69, no. 1, pp. 149–163, Jan. 2021.

[11] M. Careem, S. Chakaraborty, A. Dutta, D. Saha, and G. Hellbourg, "Spectrum sharing via collaborative RFI cancellation for radio astronomy," in *IEEE Int. Symp. Dynamic Spectr. Access Netw.*, Dec. 2021, pp. 97–104.

[12] Z. Zou, X. Wei, D. Saha, A. Dutta, and G. Hellbourg, "SCISRS: Signal cancellation using intelligent surfaces for radio astronomy services," in *IEEE Global Commun. Conf.*, Dec. 2022, pp. 4238–4243.

[13] *Physical layer procedures for data*, 3GPP Technical Specification 38.214, Jul. 2020.

[14] OpenStreetMap contributors. (2024) OpenStreetMap. [Online]. Available: https://www.openstreetmap.org

[15] Panel on Frequency Allocations and Spectrum Protection for Scientific Uses, *Handbook of frequency allocations and spectrum protection for scientific uses*. National Academies of Sciences Engineering and Medicine and others, 2015.

[16] Z.-q. Luo, W.-k. Ma, A. M.-c. So, Y. Ye, and S. Zhang, "Semidefinite relaxation of quadratic optimization problems," *IEEE Signal Process. Mag.*, vol. 27, no. 3, pp. 20–34, Apr. 2010.

[17] N. Sidiropoulos, T. Davidson, and Z.-Q. Luo, "Transmit beamforming for physical-layer multicasting," *IEEE Trans. Signal Process.*, vol. 54, no. 6, pp. 2239–2251, Jun. 2006.

[18] M. Grant and S. Boyd. (2014, Mar.) CVX: Matlab software for disciplined convex programming, version 2.1. [Online]. Available: https://cvxr.com/cvx

[19] ——, "Graph implementations for nonsmooth convex programs," in *Recent Advances in Learning and Control*. Springer-Verlag Limited, 2008, pp. 95–110.

[20] *Study on channel model for frequencies from 0.5 to 100 GHz*, 3GPP Technical Report 38.901, Nov. 2020.